Pharm Res (2015) 32:2950–2959
DOI 10.1007/s11095-015-1676-4

RESEARCH PAPER

Particle Image Velocimetry Evaluation of Fluid Flow Profiles in USP 4 Flow-Through Dissolution Cells

Hiroyuki Yoshida[1] • Akemi Kuwana[1] • Hiroko Shibata[1] • Ken-ichi Izutsu[1] • Yukihiro Goda[1]

Received: 13 November 2014 / Accepted: 10 March 2015 / Published online: 20 March 2015

ABSTRACT

Purpose To evaluate fluid flow profiles in the flow-through cell (FTC, USP apparatus 4) system with pulsatile and non-pulsatile pumps.

Methods Instantaneous velocity vectors in the dissolution cells were obtained from images sequentially captured by a particle image velocimetry (PIV) system. The data were sorted to follow the pump pulse cycle.

Results The analysis showed changes in the flow profiles during a pump pulse (0.5 s) at a 0.025-s interval in two sizes of cells installed in the FTC system. Supplying a slow flow from the pulsatile pump induced instantaneous downward (inner layer) and upward (outer layer) flow in the larger cell during the suction phase. Analysis at varied medium and cell temperatures strongly suggested a contribution of natural convection to the complex flow caused by relatively high cell temperature. Uniform upward flow was observed in other cells and flow rate conditions. The time-averaged vertical velocities in the cells were similar in the pulsatile and non-pulsatile pump systems.

Conclusions The PIV analysis provides information on how flow rate and pump pulse affect fluid flow profiles at multiple points in flow-through dissolution cells. An appropriate temperature control should reduce the complex flow of the medium in the FTC system.

KEY WORDS dissolution testing · flow-through cell system · hydrodynamics · particle image velocimetry · pulsatile pump

Electronic supplementary material The online version of this article (doi:10.1007/s11095-015-1676-4) contains supplementary material, which is available to authorized users.

✉ Hiroyuki Yoshida
h.yoshida@nihs.go.jp

[1] Division of Drugs, National Institute of Health Sciences, Kamiyoga 1-18-1, Setagaya-ku Tokyo 158-8501, Japan

ABBREVIATIONS

CFD	Computational fluid dynamics
EP	European Pharmacopoeia
FTC	Flow-through cell
i.d	Inside diameter
JP	Japanese Pharmacopoeia
MRI	Magnetic resonance imaging
PIV	Particle imaging velocimetry
P-T_p	Processing phase time
T_p	Time phase of pump
USP	United States Pharmacopeia

INTRODUCTION

Dissolution tests are widely used to evaluate drug release rates from pharmaceutical dosage forms during early and late stages of product development. A flow-through cell (FTC) dissolution system is one of the dissolution methods listed in European Pharmacopoeia (EP), United States Pharmacopeia (USP), and Japanese Pharmacopoeia (JP). The FTC system is often used to assess dissolution rates of highly functional dosage forms, e.g., enteric-coated, modified-release, and extended-release products. Their capability to maintain the sink condition by constantly replenishing the dissolution media (1), and the relative ease in changing media during the dissolution test are apparent advantages of the FTC system (2). The Pharmacopoeias specify two sizes of dissolution cells for the dissolution test of tablet formulations. They also require use of a non-pulsatile and pulsatile pump with certain sinusoidal waves (120±10 pulse/min). Several studies on the FTC system indicated critical factors affecting the dissolution profiles of test formulations, including flow rate (3,4), size of glass beads, cell temperature, tablet orientation, and level of deaeration (5).

The hydrodynamic flow of test media is recognized as a predominant factor affecting the dissolution rate. For

example, filling the conical part of the dissolution cell with 1-mm glass beads also alters the dissolution rate of tablets by changing the flow profile (4). The effect of hydrodynamic flow on the dissolution rate in the FTC and other (e.g., rotating basket and paddle) testing methods is explained by changes in the degree of mechanical stress (6–8). The hydrodynamic flow profiles in dissolution apparatus are mainly studied in two ways, specifically, modeling (simulation) and experimental measurement (visualization). The simulation of hydrodynamic flow, known as computational fluid dynamics (CFD), was often used to obtain the fluid velocity in vessels (9–14) and flow-through dissolution cells. Kakhi reported the occurrence of instantaneous downward flow near the tablet, caused by different water pressure between the upper and lower layers in the dissolution cells (15,16). D'Arcy *et.al.* showed complex flow profiles in larger dissolution cells involving natural convection at low flow rates (17,18). The CFD method provides detailed information on flow profiles at a relatively short interval; however, the simulation is based on some assumptions. Shiko *et.al.* reported the application of a magnetic resonance imaging (MRI) technique for the visualization of hydrodynamic flow profiles in a flow-through dissolution cell (19,20). The MRI technique provided quantitative information on the fluid velocities in dissolution cells, including the presence of natural convection induced by the temperature gradient in the test medium. Complex data analysis and the necessity for the study to remove the flow-through dissolution cell from the system to insert the narrow MRI probe hamper the wide application of the method in evaluating flow profiles in practical conditions.

A particle image velocimetry (PIV) system is representative of methods by which the dynamics of air and liquids can be obtained from sequentially captured images of the instantaneous movement of particles in a two-dimensional (2-D) field. The application of the method for the analysis of flow profiles in dissolution vessels has been previously reported (12,13). The availability of fluid profiles from flow-through dissolution cells installed in an actual apparatus setting would enable clarification of factors required to improve the testing method.

We studied the effects of dissolution cell size, flow rate, and pump type, which were possible variables under standard conditions stated in the Pharmacopeias, on the fluid flow profiles in a conventional FTC system using the PIV method. Because short pump pulses do not enable multiple flow data to be acquired at the low-frequency frame rate (max. 6 Hz) of the camera used in the study, the instantaneous velocity data were sampled at time points over several pump cycles. It was assumed that the flow patterns are repeated after each pump pulse so that the flow behavior over an entire cycle could be patched together using data sampled from multiple pump cycles. The data processing provided the sequential changes in the hydrodynamic flow during a pump pulse over a short time interval. We also evaluated the possible effect of temperature gradient in the dissolution cell on these profiles to assess the appropriate test condition for the FTC system.

MATERIALS AND METHODS

FTC System

A flow-through dissolution test system (CE 7 smart; SOTAX AG, Basel, Switzerland) with a pulsatile pump (CP 7–35; SOTAX AG) was used in open-loop mode. The pump was validated to meet JP and USP standards, which stipulate that a pump has an average flow rate with a 5% variation and a pulsation of 120 ± 10 pulse/min in the pulsatile flow. We confirmed compliance of the pump pulse by manual measurements (120 ± 0 pulse/min, $n = 3$). As a non-pulsatile pump, a double syringe pump equipped in a FTC-1 system (Japan Machinery Company, Tokyo, Japan) was connected to the flow-through dissolution cell in the CE 7 system without changing the peripheral devices (Fig. 1(a)). Following the manufacturer's instruction manual, routine validation and confirmation of the flow rate accuracy (±2%) were performed before use. Pulsatile flow with semi-sine wave and constant flow were given by the pulsatile and non-pulsatile pumps, respectively (Fig. 1(b)). The fluid flow was studied in two SOTAX dissolution cells for tablets with inside diameter (i.d.) of 22.6 mm and 12 mm. A 5-mm ruby bead was set on the bottom of the dissolution cell, and the conical space of the cell was filled with about 6.25 g (22.6-mm i.d. cell) or about 0.75 g (12-mm i.d. cell) of 1-mm glass beads. Two layers of glass filters with pore sizes 0.7 μm and 2.7 μm (Whatman Ltd., Maidstone, UK) were set at the outlet of the cell. A water bath in the CE 7 system was used to control the temperature of the dissolution medium before entering the cell and that of the circulation water for the jacket covering the cell. The fluid temperature at the cell inlet was regulated at 37 ± 0.5°C, unless otherwise stated, by manually setting the water bath at varied temperatures depending on the fluid flow rate, to compensate the fluid cooling in the tube between the water bath and the cell inlet, following the manufacturer's instruction manual. For example, the water bath was kept at 40.0°C (4 mL/min), 38.2°C (8 mL/min) or 37.8°C (16 mL/min) to achieve the designated fluid temperature (37 ± 0.5°C). The fluid temperature at the cell inlet and in the water bath was measured using a thermometer connected to the CE 7 system.

For visualization of the water stream, a spoonful of nylon beads (5 μm, Daicel-Evonik Ltd., Tokyo, Japan), representative tracer particles in the PIV system, was suspended in deaerated distilled water by continuous stirring in a glass bottle (1000 mL). The significantly low sedimentation rate of the nylon beads in the water, calculated using Stokes' law (3.9E–4 mm/s), is ignored. The beads suspension was introduced

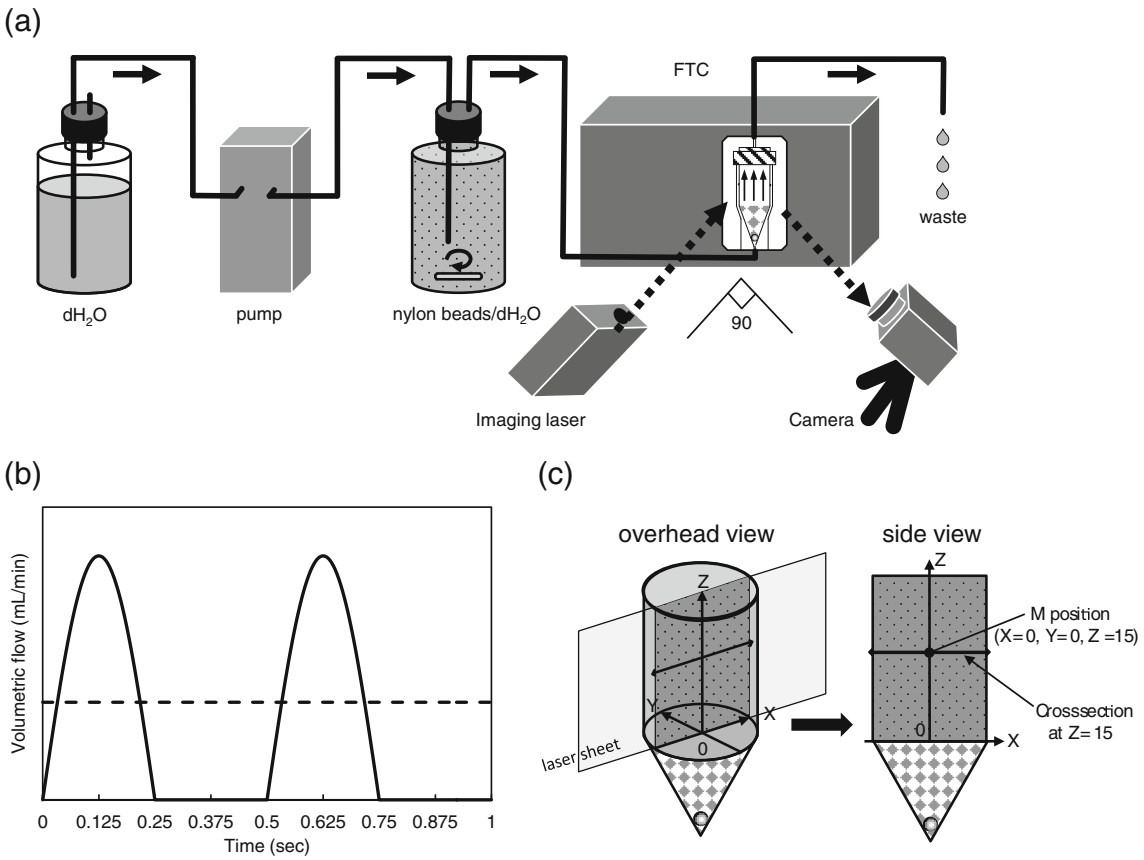

Fig. 1 Schematics of (**a**) the PIV and flow-through cell system, (**b**) the volumetric flow periodicity from pulsatile (*solid line*) and non-pulsatile (*dashed line*) pumps, and (**c**) the coordinate system used in recording data from the cell.

into the FTC system using a pulsatile or non-pulsatile pump (Fig. 1(a)).

Positions in the flow-through dissolution cells are given by horizontal (X-axis) and vertical (Z-axis) coordinates with the origin at the center of the flat surface of the cone (Fig. 1(c)). In this study, fluid velocities at a particular position where the tablets are usually held during the dissolution test (referred to as the "M position", X=0 mm, Z=15 mm) and other positions in the cross-sectional plane at Z=15 mm in both 12-mm i.d. and 22.6-mm i.d. cells were studied (Fig. 1(c)).

Visualization of Fluid Dynamics

Fluid flow profiles in a flow-through dissolution cell were obtained using the PIV method. A VisiVector LS12-2D system composed of a high-speed imaging laser and a high-performance digital camera (Firefly Laser and PIV Cam S QE CCD camera; Oxford Lasers Ltd., Oxon, UK) were used to capture sequential pairs of images of the 2-D velocity field. The imaging laser in the experimental setup (Fig. 1(a)) emits two pulses of 808–815-nm infrared radiation to create a thin vertical light sheet (approximately 1 mm thick) in one laser triggering. Use of an infrared laser has an advantage in avoiding contamination from environmental lights. The orientation of the laser sheet was adjusted to cross the center of the dissolution cell. The duration of laser beam radiation was set for 50 μs at a pulse separation of 9 ms between two sequential pulses in a laser trigger. The time interval of the laser triggers was set to 0.675 s (1.481 Hz); the frame rate of the imaging camera was controlled to synchronize with the laser trigger. One hundred paired images were captured 20 min after starting the pump flow.

Analysis of Fluid Flow Property

The instantaneous fluid movements at multiple positions were obtained by cross-correlating each pair of images captured within a short time span (9 ms). Paired images were analyzed using VidPIV software version 4.6xp (Oxford Lasers Ltd.), which performs cross-correlation, velocity and noise filtering, and averaging. To obtain fluid flow profiles over an entire pump cycle, a set of 100 pairs of images was obtained from multiple pump cycles in a 0.675-s interval. Because the pump cycles were repeated in a 0.5-s interval, appropriate multiples of the pump cycle time (0.5 s) were subtracted from the measurement time to obtain the "processing" phase time ($0\ s \le P - T_p \le 0.5\ s$) of the data point (Fig. 2(a)). Having assumed that flow patterns are repetitive and fluid flow profiles can be

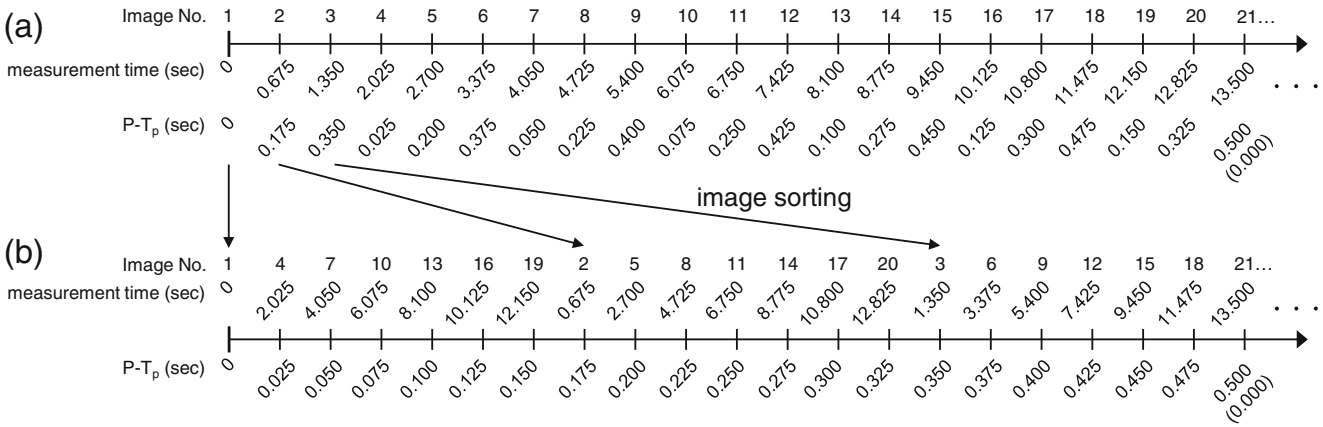

Fig. 2 Illustrations of sorting of sequentially captured images. (**a**) 100 sequential pairs of images were captured at a 0.675-s interval. (**b**) Images were sorted following their P-T_p in the 0.5-s pump pulse, resulting in a set of 20 images at a 0.025-s interval.

patched, sorting of the instantaneous fluid velocity data following the P-T_p gives a periodic data set of 20 points in the pump-pulse phase (Fig. 2(b), five cycles from 100 pairs of image). Because of the independent function of the pump pulse and the laser trigger, the P-T_p starts at arbitrary times in the pump cycle for each measurement. Hence, the pump time (T_p) for the analysis of the fluid flow property is obtained by defining the time when the fluid velocity at the M position shows maximum value as T_p=0.125 s to give a better comparison of the change in flow between measurements. The value was chosen because the discharge rate, assumed sinusoidal, attains its maximum value at T_p=0.125 s (15).

RESULTS

Visualization of Fluid Flow Profiles in a 12-mm i.d. Dissolution Cell Using a Pulsatile Pump

Figure 3 shows the fluid flow profiles for a 12-mm i.d. cell at the flow rate of 4 mL/min shown as the instantaneous velocity vectors in the vertical 2-D field. The multiple arrows were uniformly facing upward in all areas of the dissolution cell at T_p=0.125 s (Fig. 3(a)). In contrast, fluid velocities were constrained and the vectors were randomly directed at time point T_p=0.375 s (Fig. 3(b)). Figure 4 shows the changes in the vertical (Z-axis) flow velocity during the pump cycle (0.025-s interval) at the M position for 12-mm i.d. cell at flow rates of 4, 8, and 16 mL/min. A smaller change in fluid velocity over $0.250 \le T_p \le 0.475$ s corresponds to a suction phase in the pump cycle. The Z-axial velocity at the peak of discharge (T_p=0.125 s) varied with the average flow rate of pulsatile pump. The results indicate that after sorting of the velocity data the PIV analysis can identify changes in medium flow in the FTC during a pump cycle. Also, the small fluid velocity during the suction phase signifies that the ruby bead acts as a check valve.

Figure 5 shows the time-dependent change in the vertical flow during a pump cycle in each different X-axis position in a cross-sectional plane (15 mm height). The graphs indicate similar flow rates at the cell center and outer region at the low flow rate of 4 mL/min (Fig. 5(a)). The uniform fluid flow can be observed in supplementary video 1. Flow uniformly directed upward was also observed over all areas at flow rates of 8 and 16 mL/min (data not shown). At these higher flow rates, analysis of these cells show faster local flow near the center of the dissolution cell (X=0 mm) compared with the flow at the outer region.

Visualization of Fluid Flow Profiles in a 22.6-mm i.d. Dissolution Cell Using a Pulsatile Pump

Next, we investigated fluid flows in the larger (22.6-mm i.d.) cell at flow rates of 4, 8, and 16 mL/min using the pulsatile pump. Figure 6 shows the instantaneous velocity vectors in the vertical 2-D field in 22.6-mm i.d. cell (4 mL/min) at the discharge (T_p=0.125 s) and suction (T_p=0.375 s) phases. These figures clearly show the variation in the flow depending on the pump phase and the area (Fig. 6). The test medium flows upward at T_p=0.125 s. The velocity of the fluid near the inner wall was higher than that in the center of the dissolution cell (Fig. 6(a)). The medium around the center moves downward during the suction phase (T_p=0.375 s) while an upward flow is observed in the outer region (Fig. 6(b)). Figure 7 indicates vertical fluid flow velocities at the M position of the 22.6-mm i.d. cell obtained for all three flow rates. While the values are positive during the discharge phase ($0 \le T_p \le 0.200$ s), the values remain constant and negative during the suction phase ($0.225\text{ s} \le T_p \le 0.475$ s) at flow rates of 4 and 8 mL/min. The fluid flow profiles at the different horizontal positions clearly indicate temporary downward flow near the center of the dissolution cells (Fig. 8(a) and (b)). The figures also indicate faster vertical fluid flow in the outer area compared with those in the cell centers at all time phases. The downward flow

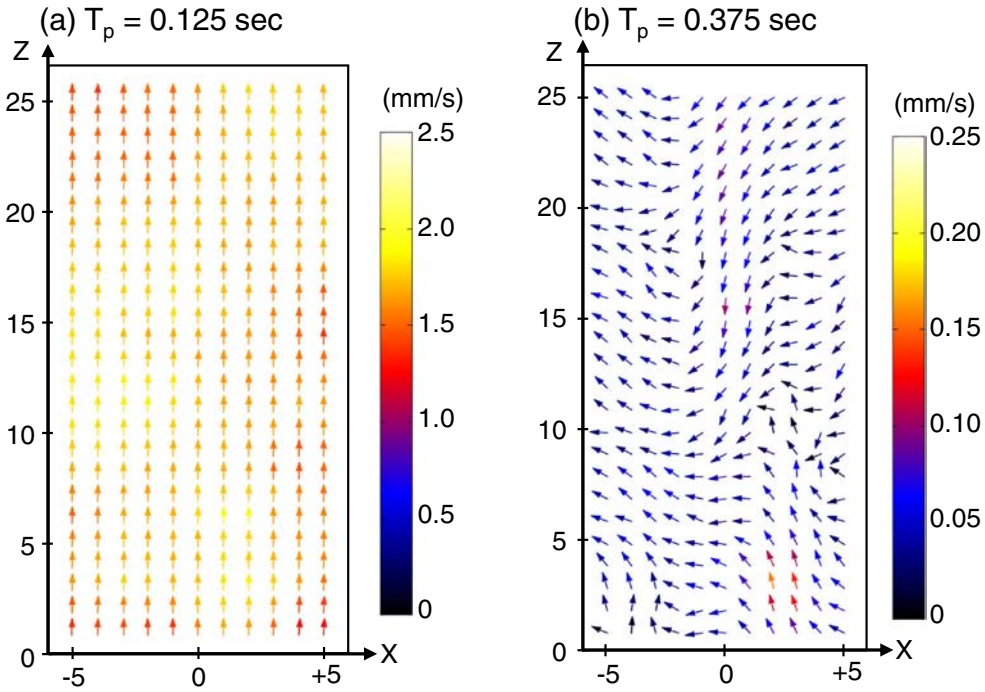

Fig. 3 Instantaneous fluid velocity vectors in vertical 2-D field at (**a**) discharge ($T_p = 0.125$ s) and (b) suction ($T_p = 0.375$ s) phases using a pulsatile pump (flow rate: 4 mL/min, 12 mm i.d. dissolution cell). The color scale corresponds to the absolute velocity. Each result represents the mean of three identical experiments.

around the center of the cells was not observed at flow rates of 16 mL/min (Fig. 8(c)).

Comparison of Fluid Flow Profiles in a Dissolution Cell Between the Use of Pulsatile and Non-Pulsatile Pumps

EP, USP, and JP prescribe the use of non-pulsatile or certain pulsatile pumps in FTC tests; however, limited information is available on how the pump types affect flow profiles and dissolution of formulations in the FTC system. We compared the fluid dynamics in the system using the pulsatile and non-pulsatile pumps. Figure 9 shows the change in volumetric flow rate during a pump cycle at a flow rate of 8 mL/min in 12 and 22.6-mm i.d. cells. The volumetric flow rates were calculated by integrating over the vertical velocity at $Z = 15$ mm shown in Figs. 5(b) and 8(b) with respect to X-axis. The much smaller variation in the volumetric flow rate indicates supply of a non-pulsatile flow into both 12 and 22.6-mm i.d. dissolution cells (Fig. 9). In addition, the velocities using a non-pulsatile pump were comparable to the setting flow rate of 8 mL/min in both size of cells.

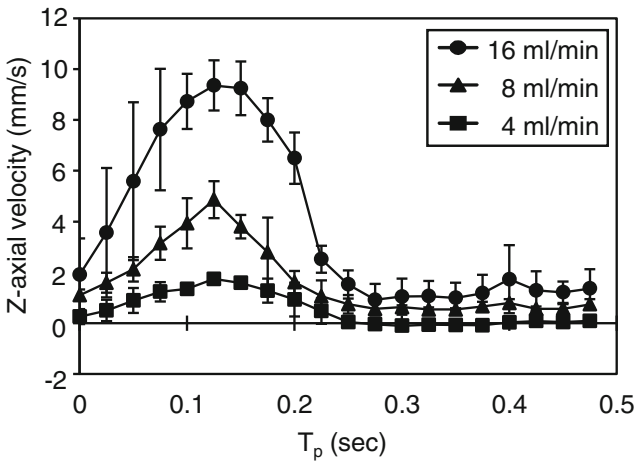

Fig. 4 Vertical (Z-axial) flow velocities at the M position ($X = 0$ mm, $Z = 15$ mm) during a pump pulse (flow rate: 4–16 mL/min, 12-mm i.d. dissolution cell). Each result represents the mean ± SD of three identical experiments.

Figure 10 indicates time-averaged flow profiles obtained for the horizontal cross-section at $Z = 15$ mm in the systems using the pulsatile and non-pulsatile pumps (flow rates: 4–16 mL/min). To compare the fluid flow profiles using these pumps, the averaged vertical velocities over a 20 time phase (i.e., one pump pulse) in each sampled X-axis position were plotted. Many curves in the figure showed similar profiles in the average vertical flow in the systems using the pulsatile and non-pulsatile pumps (Fig. 10). The profile in the non-pulsatile system also shows faster fluid flow in the outer region at flow rates of 4 and 8 mL/min in the 22.6-mm i.d. cell (Fig. 10(d) and (e)). These results indicated that, despite the periodic change in fluid velocity in the pulsatile pump, there was no apparent difference in the time-averaged fluid flow profiles between the pulsatile and non-pulsatile pumps.

Effect of Temperature Gradient in the Test Medium on Fluid Flow Profiles

A previous study involving an MRI experiment (19) discussed a possible contribution from the temperature gradient in the

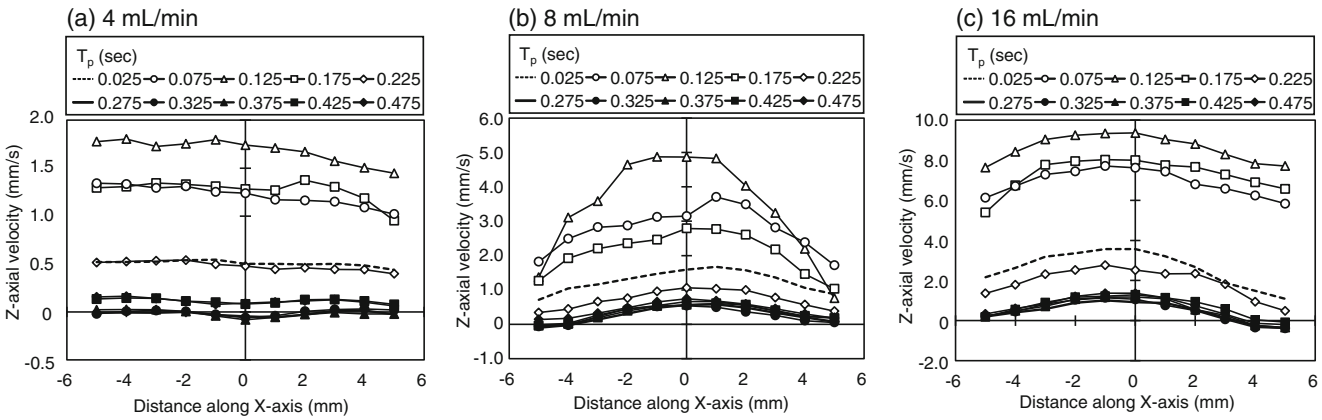

Fig. 5 Changes in profiles of vertical fluid velocity during a pump cycle in each different X-axis position in the cross-section ($Z = 15$ mm) (flow rate: 4–16 mL/min, 12-mm i.d. dissolution cell). Each result represents the mean of three identical experiments.

test medium in the flow-through dissolution cells and a corresponding natural convection as the cause of the instantaneous downward flow observed in some systems. In the present FTC system, the temperature gradient also has the potential to induce natural convection strongly affecting fluid flow profile. The temperature of the test medium in the particular FTC system cell is controlled both by the supplied medium and the circulation water jacket holding the cell (Fig. 11(a)). The possible differences in temperature between the medium entering the cell and the inner cell surface should result in the temperature gradient inducing the natural convection. We thus intentionally altered these parameters to clarify the cause of the downward flow observed in the 22.6-mm i.d. cell (4 mL/min). Figure 12(a) indicates flow profiles obtained under conditions that possibly reduce the temperature gradients. Absence of a water-bath temperature control kept both the test medium at the cell inlet and the circulation water at the same temperature (26.7°C, Table I, Fig. 11(b)). The PIV analysis indicated uniform upward flow over a wide area of the cell (Fig. 12(a)). Raising the water-bath temperature (30.0, 35.0°C) reduced the averaged vertical velocity in the center, and concomitantly increased the flow near the inner wall. The higher water-bath temperature increased the temperature difference from that of the test medium at the cell inlet (Table I, Fig. 11(a)). This strongly suggests a contribution from the temperature difference between the cell wall and introducing media, and hence the resulting temperature gradient of the media in the center and outer region of the cell, in generating natural convection in the dissolution cell.

In another experiment, we introduced conditions by which the medium entering the cell has a higher temperature compared with the water temperature in the cell jacket. We heated

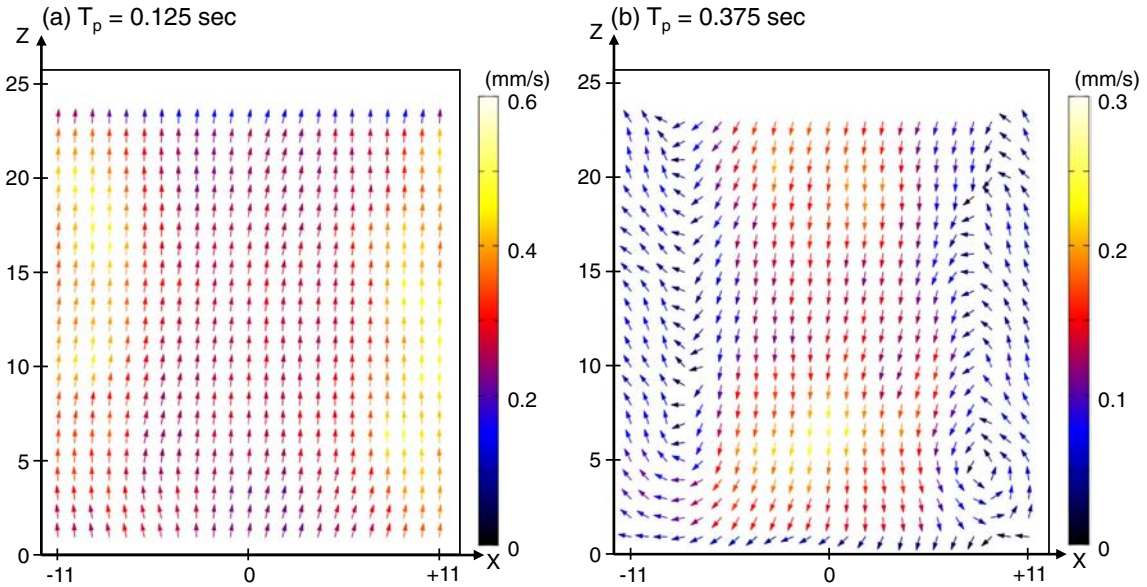

Fig. 6 Instantaneous fluid velocity vectors in a vertical 2-D field at (**a**) discharge ($T_p = 0.125$ s) and (**b**) suction ($T_p = 0.375$ s) phases using a pulsatile pump (flow rate: 4 mL/min, 22.6 mm i.d. dissolution cell). The color scale corresponds to the absolute velocity. Each result represents the mean of three identical experiments.

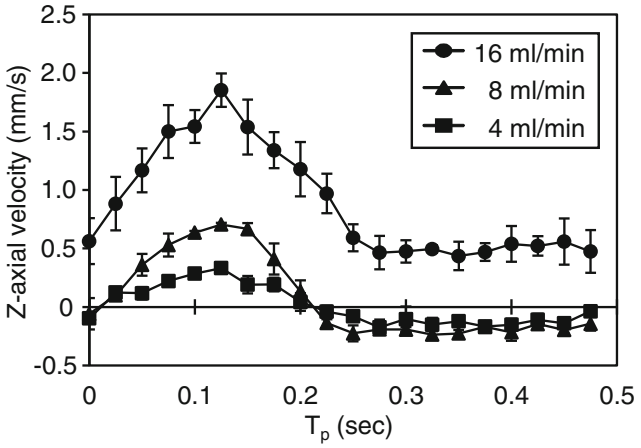

Fig. 7 Vertical fluid velocities at the M position ($X=0$ mm, $Z=15$ mm) during a pump pulse (flow rate: 4–16 mL/min, 22.6-mm i.d. dissolution cell). Each result represents the mean ± SD of three identical experiments.

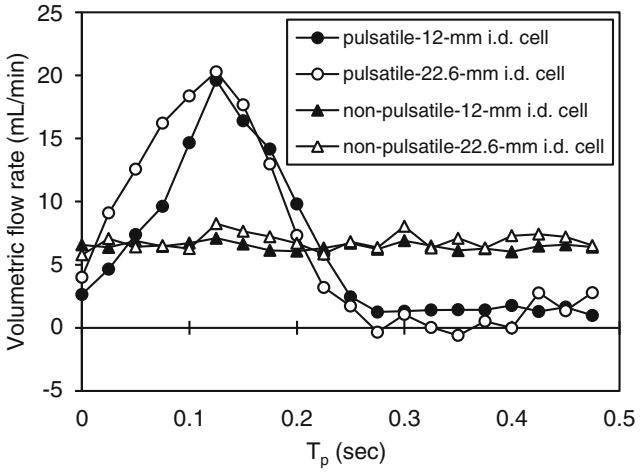

Fig. 9 Change in volumetric flow rate during a complete stroke of pulsatile pump (flow rate: 8 mL/min, 12 and 22.6-mm i.d. dissolution cell). The volumetric flow rates were calculated by integrating over the vertical velocity at $Z=15$ mm shown in Figs. 5 and 8 with respect to the X-axis. Changes in the volumetric flow rate in the non-pulse pump system during the period are also shown. Each result represents the mean of three identical experiments.

only the inflowing test medium to maintain a temperature of 37±0.5°C by setting the bath temperature at 40.0°C, and closing the water circulation heating the cell jacket (Fig. 11(c)). Interestingly, the PIV analysis gave a continuous downward flow in the outer region and a faster vertical flow inside (Fig. 12(b)). These results demonstrated that the induced reverse temperature gradient induced the downward flow of the medium at different positions in the 22.6-mm i.d. cell at the lower flow rate.

DISCUSSION

The PIV analysis allowed visualization of short-term (during a pulse) and long-term (averaged) fluid flow profiles at multiple points inside the dissolution cell installed in a FTC apparatus. The fluid flow inside the cells followed the pump-pulse cycle. The visualization would be a powerful tool to understand the effect of hydrodynamic flow on the dissolution rate of formulations in the flow-through dissolution cell (3,4,7). The advantage of the PIV system is its applicability to the FTC system without changing the FTC system composition, which results in the evaluation of real flow profiles. Our study demonstrated a large contribution to the temperature gradient in the media that partially depends on the composition of the FTC system and on the fluid flow property. In relation to the CFD study (15), the peak velocity at discharge phase (T_p= 0.125 s) at a flow rate of 16 mL/min in 22.6-mm i.d. cell in the current work was about two-thirds (about 2.0 mm/s vs 3.0 mm/s). In contrast, the flow velocities at $T_p=0.625$ or 0.1875 s were comparable. Isothermal condition in CFD system would be one reason for these differences in fluid-flow profiles. Moreover, the results support previous reports on the presence of a downward flow at lower flow rates in the MRI analysis. The natural convection induces faster upward flow in the warmer area and a concomitant slower or

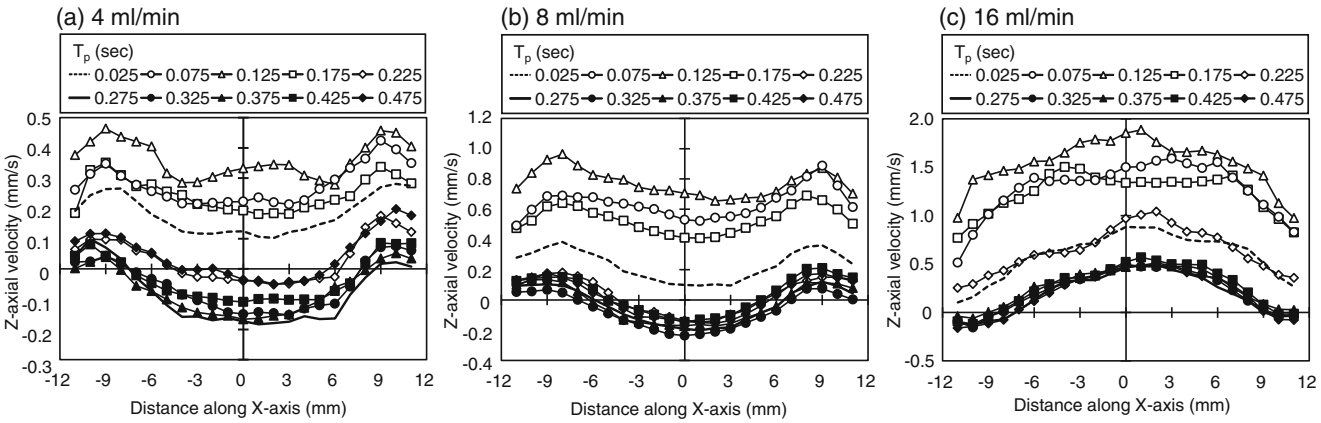

Fig. 8 Changes in profiles of vertical fluid velocity during a pump cycle in each different X-axis position in the cross-section ($Z=15$ mm) (flow rate: 4–16 mL/min, 22.6-mm i.d. dissolution cell). Each result represents the mean of three identical experiments.

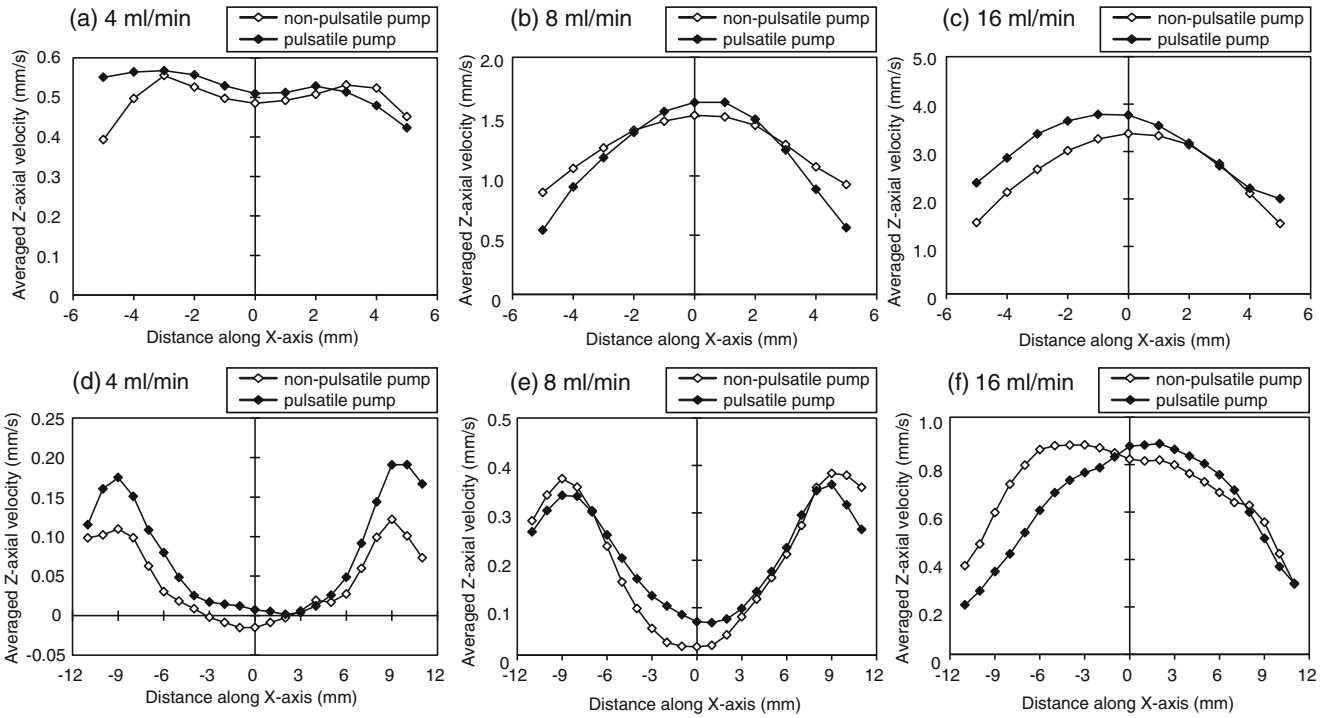

Fig. 10 Comparison of averaged Z-axial fluid velocities at several positions in cross-section ($Z = 15$ mm) using pulsatile and non-pulsatile pumps (flow rate: 4–16 mL/min with dissolution cell of (upper) 12-mm and (lower) 22.6-mm i.d.). The Z-axial velocities in 20 time phases over one complete pump cycle were averaged and plotted. Each result represents the mean of three identical experiments.

downward flow in the cooler region. However, the area flowing downward direction in the present study was different from that in the MRI analysis. The constant downward flow near the inner wall due to the cooler cell wall, as indicated by the flow profile shown in Fig. 12(b), was reported in the larger cells (19). Alteration of the system setting required for the MRI analysis (e.g., removal of the dissolution cell from the system and use of adhesive insulating foam instead of a water jacket) can explain some differences in the observed flow profiles between the studies.

The observed difference in the instantaneous flow between the cell center and outer layer, including the occurrence of the

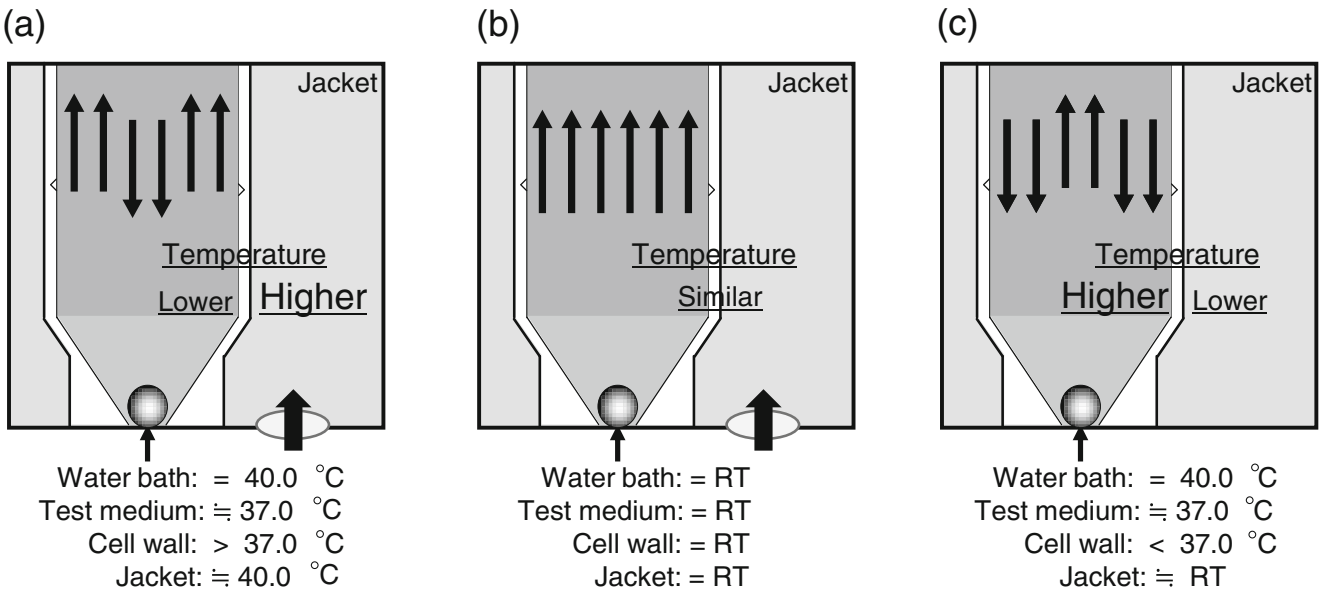

Fig. 11 Schematics of the system operation at different test medium and water bath temperature settings. (**a**) Warmed test medium and water for a jacket were introduced into the system. (**b**) Test medium and water at room temperature (RT) were introduced into the system. (**c**) Water jacket was filled with water at RT and warmed test medium was introduced into the cell. The water circulation for water jacket was unactuated.

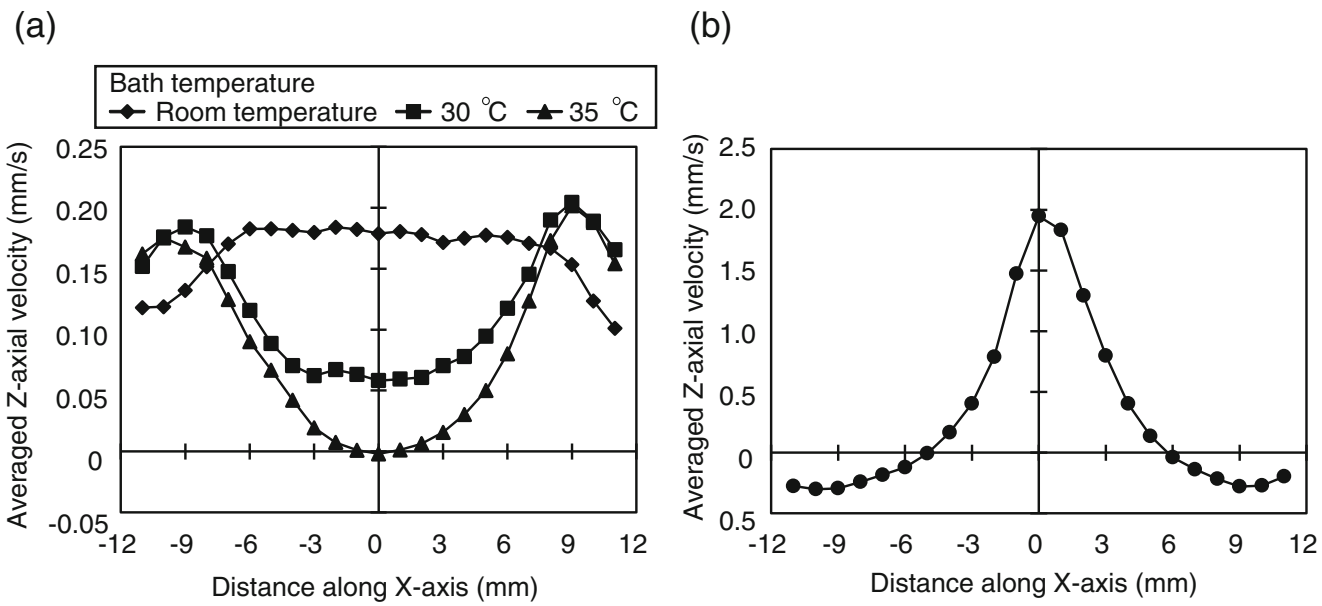

Fig. 12 Effect of water temperature in the water jacket and in the dissolution cells on the averaged vertical fluid velocities at several positions in the cross-section ($Z = 15$ mm) using pulsatile pump (flow rate: 4 mL/min, 22.6-mm i.d. dissolution cell). (**a**) The water bath temperature was set to 30.0, 35.0°C, or room temperature (no heating). (**b**) The water bath temperature was set to 40.0°C and the water circulation was stopped. The vertical fluid velocities in 20 time phases over one complete pump cycle were averaged and plotted. Each result represents the mean of three identical experiments.

downward flow, can be reduced by minimizing the temperature gradient of the medium that causes the natural convection in the cell. It is possible that the normal setting of the apparatus keeps the temperature of the test medium near the inner wall warmer than that around the center of the dissolution cell in the FTC system. The temperature of the test medium in the dissolution cells is controlled by both preheating with the water bath and the water jacket holding the cells. The test medium pre-heated in the water bath was cooled in fine-bore tubes that pass through before entering the dissolution cells. The temperature drop should be more apparent at lower flow rates. In contrast, the circulation water should lose less heat before entering the cell jacket because the water flows through one large-bore tube from the water bath to the main unit of FTC system at higher flow rates (390 mL/min, measured), immediately before being channeled through the seven short tubes connected to the water jacket. Possible cooler medium entering the cell through the long thin tube and warmer outer layer medium contacting the higher temperature cell wall should induce a temperature gradient at low flow rates. Moreover, the calculated cross-sectional velocities under these conditions were exceptionally low; therefore, the effect of natural convection should become apparent at the lower flow rate (17). The apparent dependence of the flow profile on the medium and cell jacket temperatures emphasizes the relevance of an appropriate temperature control (e.g., use of a thermal insulator) to establish robust flow-through dissolution tests. The complex flow can explain the limited effect of flow rates on dissolution profiles in the tests using the 22.6-mm i.d. dissolution cell (4,21,22).

Table I Set and Measured Temperature in FTC System 20-min After Starting of Pump at Flow Rate of 4 ml/min

Setting temperature of water bath (°C)	Not heating	30.0	35.0	40.0
Circulation water in water bath (°C)	26.7	30.0	35.0	40.0
Test medium at cell inlet (°C)	26.7	29.4	33.6	37.0

The flow-through dissolution test standardized in USP, EP, and JP permits the use of pulsatile and non-pulsatile pumps. To our knowledge, there are few studies comparing the hydrodynamic properties in the dissolution cell between the pulsatile and non-pulsatile pumps. The systems with the pulsatile and non-pulsatile pumps showed similar averaged vertical flow profiles in this study. These similar averaged flow profiles, however, cannot assure the same dissolution profiles of test formulations in the systems with these pumps. Varied flows and associated pressure changes at the formulation surface during the pump pulse can affect the dissolution profile of the formulation. The regional instantaneous downward flow observed in some flow conditions in the pulsatile pump system can also affect dissolution. Parallel studies of the hydrodynamic property and dissolution profiles would clarify their relationship. Moreover, two types of the pulsatile pump sending a semi-sine wave or a full sine wave were reported (23). The former is the pump we used in the current study, but the latter needs to be investigated. The effect of other conditions such as

glass-bead size on the fluid flow profiles and the formulation dissolution are also intriguing topics for further elucidation (5,24).

CONCLUSIONS

The fluid flow profiles in flow-through dissolution cells were evaluated using PIV analysis. Availability of precise flow information in actual apparatus settings would enable robust flow-through dissolution tests to be established. Better control of the medium temperature should reduce the irregular flow caused by natural convection. The effects of sample formulations on the flow profile and how they affect the dissolution are intriguing topics that require elucidation.

ACKNOWLEDGMENTS AND DISCLOSURES

This work is partly supported by a Health and Labour Sciences Research Grant from the Ministry of Health, Labour, and Welfare of Japan.

REFERENCES

1. Moller H, Wirbitzki E. Regulatory aspects of modified release dosage forms: special cases of dissolution testing using the flow-through system. Boll Chim Farm. 1993;132(4):105–15.
2. Fotaki N, Reppas C. The Flow Through Cell Methodology in the Evaluation of Intralumenal Drug Release Characteristics. Dissolut Technol. 2005;12(2):17–21.
3. Gao Z. In vitro dissolution testing with flow-through method: a technical note. AAPS PharmSciTech. 2009;10(4):1401–5.
4. Bielen N. Performance of USP calibrator tablets in flow-through cell apparatus. Int J Pharm. 2002;233(1–2):123–9.
5. Eaton JW, Tran D, Hauck WW, Stippler ES. Development of a performance verification test for USP apparatus 4. Pharm Res. 2012;29(2):345–51.
6. Kamba M, Seta Y, Takeda N, Hamaura T, Kusai A, Nakane H, *et al.* Measurement of agitation force in dissolution test and mechanical destructive force in disintegration test. Int J Pharm. 2003;250(1):99–109.
7. Morihara M, Aoyagi N, Kaniwa N, Katori N, Kojim S. Hydrodynamic flows around tablets in different pharmacopeial dissolution tests. Drug Dev Ind Pharm. 2002;28(6):655–62.
8. Wennergren B, Lindberg J, Nicklasson M, Nilsson G, Nyberg G, Ahlgren R, *et al.* A collaborative in vitro dissolution study: comparing the flow-through method with the USP paddle method using USP prednisone calibrator tablets. Int J Pharm. 1989;53(1):35–41.
9. Bai G, Wang Y, Armenante PM. Velocity profiles and shear strain rate variability in the USP Dissolution Testing Apparatus 2 at different impeller agitation speeds. Int J Pharm. 2011;403(1–2):1–14.
10. Baxter JL, Kukura J, Muzzio FJ. Shear-induced variability in the United States Pharmacopeia Apparatus 2: modifications to the existing system. AAPS J. 2005;7(4):E857–864.
11. Baxter JL, Kukura J, Muzzio FJ. Hydrodynamics-induced variability in the USP apparatus II dissolution test. Int J Pharm. 2005;292(1–2):17–28.
12. Kukura J, Arratia PE, Szalai ES, Muzzio FJ. Engineering tools for understanding the hydrodynamics of dissolution tests. Drug Dev Ind Pharm. 2003;29(2):231–9.
13. Kukura J, Baxter JL, Muzzio FJ. Shear distribution and variability in the USP Apparatus 2 under turbulent conditions. Int J Pharm. 2004;279(1–2):9–17.
14. McCarthy LG, Bradley G, Sexton JC, Corrigan OI, Healy AM. Computational fluid dynamics modeling of the paddle dissolution apparatus: agitation rate, mixing patterns, and fluid velocities. AAPS Pharm Sci Tech. 2004;5(2):e31.
15. Kakhi M. Mathematical modeling of the fluid dynamics in the flow-through cell. Int J Pharm. 2009;376(1–2):22–40.
16. Kakhi M. Classification of the flow regimes in the flow-through cell. Eur J Pharm Sci. 2009;37(5):531–44.
17. D'Arcy DM, Liu B, Bradley G, Healy AM, Corrigan OI. Hydrodynamic and species transfer simulations in the USP 4 dissolution apparatus: considerations for dissolution in a low velocity pulsing flow. Pharm Res. 2010;27(2):246–58.
18. D'Arcy DM, Liu B, Corrigan OI. Investigating the effect of solubility and density gradients on local hydrodynamics and drug dissolution in the USP 4 dissolution apparatus. Int J Pharm. 2011;419(1–2):175–85.
19. Shiko G, Gladden LF, Sederman AJ, Connolly PC, Butler JM. MRI studies of the hydrodynamics in a USP 4 dissolution testing cell. J Pharm Sci. 2011;100(3):976–91.
20. Shiko G, Sederman AJ, Gladden LF. MRI technique for the snapshot imaging of quantitative velocity maps using RARE. J Magn Reson. 2012;216:183–91.
21. Brown W. Apparatus 4 Flow Through Cell: Some Thoughts on Operational Characteristics. Dissolut Technol. 2005;12(2):28–30.
22. Cammarn SR, Sakr A. Predicting dissolution via hydrodynamics: salicylic acid tablets in flow through cell dissolution. Int J Pharm. 2000;201(2):199–209.
23. D'Arcy DM, Liu B, Persoons T, Corrigan OI. Hydrodynamic Complexity Induced by the Pulsing Flow Field in USP Dissolution Apparatus 4. Dissolut Technol. 2011;18(4):6–13.
24. Fotaki N. Flow-Through Cell Apparatus (USP Apparatus 4): Operation and Features. Dissolut Technol. 2011;18(4):46–9.